Theory of band-edge optical nonlinearities in type-I and type-II quantum-well structures

R. Binder, I. Galbraith,* and S. W. Koch
Optical Sciences Center and Physics Department, University of Arizona, Tucson, Arizona 85721
(Received 25 January 1991; revised manuscript received 15 April 1991)

A theoretical analysis of the many-body effects in the band-edge absorption spectra of highly excited type-I and type-II semiconductor quantum-well structures is presented. The situation of a homogeneous electron-hole plasma in a usual type-I structure is compared and contrasted to the situation in a type-II structure, where the electron and hole plasmas are spatially separated into adjacent layers. The plasma effects are determined through numerical solutions of a generalized Wannier equation, which accounts for dynamical exchange and screening effects as well as Pauli blocking. In the description of dynamical screening, an alternative to the so-called Shindo approximation is developed. The induced electric-field effects in the type-II systems are investigated by solving the coupled Schrödinger and Poisson equations for the charge carriers.

I. INTRODUCTION

The theory of highly excited semiconductors has long been the focus of intensive research. The influence of an electron-hole (e-h) plasma on the near-band-edge optical-absorption spectra has been studied in great detail for both bulk semiconductors and quantum-well structures.[1-4] The description of the plasma is usually based on the standard many-body theory of an electron gas, a discussion of which can be found in Ref. 5 for the case of a bulk system. The basic properties of an electron gas in a quasi-two-dimensional structure are discussed, e.g., in Ref. 6.

The general effects of an e-h plasma on the excitonic absorption have been found to be (i) plasma screening of the Coulomb interaction between the charge carriers, particularly between the attracting e-h pairs; (ii) reduction of the band gap through exchange interaction and correlation effects; and (iii) reduction of the absorption in the band-edge region, which develops into optical gain for sufficiently high plasma densities, as a consequence of phase-space filling and Pauli blocking.

In recent years the interest in optically excited semiconductors continuously increased as more and more modified and additional kinds of quantum-well structures were developed. One very important example of these systems are the so-called type-II structures. Here, the relaxation of a photoexcited e-h plasma toward a quasithermal equilibrium is accompanied by a spatial separation of the two plasma components. Such a situation arises, e.g., in the GaAs/AlAs system if the GaAs layers are sufficiently thin to push the lowest confined Γ state in the GaAs above the lowest X-like state in the AlAs layers.[7] This occurs if the GaAs thickness is less than and the AlAs thickness is greater than $\simeq 35$ Å. If the GaAs layer is replaced by (Al,Ga)As these restrictions are somewhat lifted and type-II band alignment can be achieved over a wide range of layer thicknesses.

In Fig. 1 we show the schematics of a simple GaAs/AlAs type-II quantum-well structure. The linear and nonlinear optical properties of such a system have been investigated experimentally in Ref. 8. It is shown there that the Γ-X transfer is rapid ($\simeq 500$ fs), allowing the carriers to thermalize to a quasiequilibrium distribution at the X minimum of the Brillouin zone. Since the effective mass at the X minimum is strongly anisotropic, one has to distinguish X electrons with momentum within the plane (X_{xy}) from those with momentum in growth direction (X_z). Because of the quantum confinement the minimum of the X_{xy} band is not degenerate with the minimum of the X_z band. Some controversy existed about the energetic position of those two bands for a given quantum-well structure. Conclusive studies[9] using

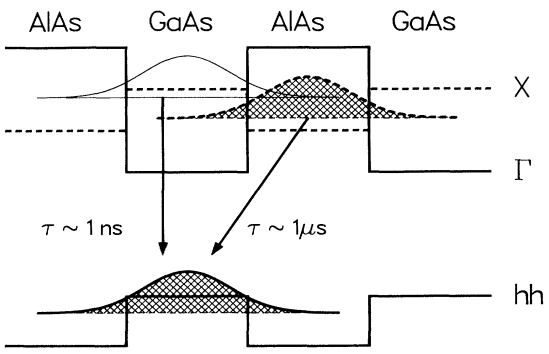

FIG. 1. Schematic of the type-II quantum-well structure. The solid line indicates the z dependence of the Γ point of the conduction and valence bands of the bulk materials, and the dashed line shows the X point of the conduction band, respectively. Indicated are also the quantum-confinement shifts of the Γ energies with the corresponding wave functions localized in the GaAs region, and the quantum confinement of the X point with the wave function localized in the AlAs layer, respectively. The arrows mark the direct (Γ-Γ) and indirect (X-Γ) radiative transitions with the corresponding typical time constants.

optically detected magnetic resonance spectroscopy determined that for 25-Å GaAs wells and AlAs thicknesses greater than about 55 Å, the lowest X minimum is X_{xy}. In samples with thinner barriers the lowest state is X_z. The crossover is attributed to the increasing confinement of the X_{xy} state overcoming the strain splitting as the AlAs thickness is reduced.

Similar to the case of n-i-p-i structures,[10] the charge separation in type-II quantum wells leads to a macroscopic electric field. In type-II systems, however, the localization of the hole plasma is solely determined by the width of the quantum well of the holes, which in our example is a 30-Å GaAs layer. The length scale of the electric-field variations is essentially determined by the distance between the holes in the GaAs layer and the electrons in the AlAs layer, respectively. Since the AlAs layer is much wider than the GaAs well, the length scale of the electric-field variations exceeds appreciably the localization scale of the hole plasma. As a consequence, the spatially indirect transitions in a type-II system, which determine the luminescence, are more affected by the electric field than the spatially direct transitions, which determine the absorption.[11] Both direct and indirect transitions are, however, strongly influenced by the many-body effects associated with the existence of a plasma. A first discussion of the many-body effects on the luminescence and absorption of highly excited type-II systems has been given in Ref. 11. It is our goal in this paper to present a detailed theory of the nonlinear optical absorption of quantum-well structures with and without e-h charge separation. To this end we focus first on the plasma effects which modify the absorption of a single GaAs layer. In Sec. II we discuss briefly the basic theoretical formulation of the problem. We use Green's-function theory which we modify and improve to allow for a unified description of type-I and type-II systems. In Sec. III we present the dynamically screened Coulomb potential employing a double-plasmon-pole approximation. In Sec. IV we finally derive the generalized Wannier equation to describe the interband polarization in type-I and type-II quantum-well systems. The derivation includes our alternative to the so-called Shindo approximation. We then analyze in Sec. V the effects of the space-charge fields caused by the spatial e-h plasma separation and its influence on the absorption spectra. In Sec. VI we show numerical results and discuss in detail the influence of the various many-body effects underlying the absorption changes of both type-I and type-II systems. A short summary and conclusion is given in Sec. VII.

II. GREEN'S-FUNCTIONS THEORY

It is generally an extremely involved theoretical task to describe a spatially inhomogeneous system like a quantum-well structure with induced electric fields due to electron-hole charge separation in type-II systems. In the following we therefore use an approximate approach which allows us to split the complete problem into two somewhat simpler parts. First, we consider the properties of a single semiconductor layer with excited electron (e) and hole (h) plasmas. To keep our treatment general we choose the e and h densities n_e and n_h as mutually independent, allowing for a description of (i) a type-I heavy-hole (hh) transition where $n_h \equiv n_{\rm hh}$ and $n_e = n_h \neq 0$; (ii) a type-I light-hole (lh) transition where $n_e \neq 0$, $n_h \equiv n_{\rm lh} = 0$ since no light holes are present at not too high excitation densities; (iii) a type-II hh transition with $n_h \equiv n_{\rm hh} \neq 0$ and $n_e = 0$, assuming ideal charge transfer of the electrons out of the GaAs layer; and (iv) a type-II lh transition where $n_h \equiv n_{\rm lh} = 0$ and $n_e = 0$. Intermediate cases will also be studied. The plasma states are chosen to be delocalized within the layer spanned by the x,y coordinates. The motion perpendicular to the layers (z direction) is localized due to the potential barriers between the layers.

Concerning the plasma theory of the GaAs layer our approach is to take into account only the lowest subband of the quantum well. This leads to a description which is formally almost identical to that of a bulk system, the main difference being that the wave vectors of the particles are restricted to the in-plane wave vectors. The usual approach to treat a nonexcited quantum well is to approximate the z dependence of the quantum-well potential as a square well. In the case of an excited system with charge transfer this square-well potential is altered by the resulting space-charge field, giving rise to shifts of the energy levels of the layer, i.e., the in-plane energy bands. These effects will be discussed in Sec. V.

An appropriate framework for the description of an optically excited semiconductor system is the nonequilibrium Green's-function approach. This is a generalization of the equilibrium Green's-function technique, which for a one-component plasma is comprehensively discussed, e.g, in Refs. 5 and 12. The Green's-function approach for highly excited bulk semiconductors in quasiequilibrium is given, e.g., in Ref. 1 and 13. The extension of the semiconductor theory to a general nonequilibrium situation has mostly been based on the Keldysh Green's-function technique[14] (see, e.g., the contributions of both Haug and Schäfer in Ref. 3, and Refs. 15 and 16; a general introduction to the Keldysh technique can be found, e.g., in Ref. 17).

In the Keldysh formalism the optical properties of a two-band semiconductor are described by the two-point Green's function $G^{cv}_{+-}(k,t_1t_2)$ (see, e.g., Ref. 3, pp. 53–81, 133–157). The band indices denote the conduction (c) and valence (v) band, respectively, and the Keldysh indices ($+-$) imply that the function is not time ordered with respect to t_1 and t_2. The Dyson equation for this Green's function has been derived for bulk semiconductors and can be found, e.g., as Eq. (3.11) in Ref. 15, or as Eq. (3.20) on p. 143 in Ref. 3. Although we are interested in layered GaAs/AlAs structures, we nevertheless start with a formally almost identical equation describing only the GaAs layer where the absorption actually takes place. The wave vector k denotes the two-dimensional in-plane wave vector. In principle, the two-point Green's function G would get two more indices specifying the subband indices of the quantum-well structure. We will, however, restrict ourselves to very thin GaAs layers, where the subband energy separation is larger than typical energies such as the exciton binding energy and the Fermi energies of the excited carriers. We

are therefore only dealing with Green's functions which involve the lowest ($l=1$) subband, and for simplicity of notation we leave out the corresponding subband labels 1,1.

Since the hh-lh splitting in thin layers is large, we neglect all Coulomb correlations which would lead to a coupling of hh and lh bands. This gives rise to a considerable simplification of the theory, as we are dealing now with two independent interband transitions (lh and hh), and we can adopt a simple two-band description for either case. hh and lh transition are distinguished by the effective masses and energy gaps, as well as by the hole distributions and densities. With these interpretations in mind, we can use Eq. (3.20) on p. 143 of Ref. 3. We start here with an equivalent equation, where no Fourier transformation with respect to time has been performed:

$$\left[i\hbar\frac{\partial}{\partial t_1}-\varepsilon_c(k)+i\hbar\frac{\partial}{\partial t_2}+\varepsilon_v(k)\right]G^{cv}_{+-}(k,t_1t_2)$$
$$=\Sigma^{cv}_f(k,t_1)G^{vv}_{+-}(k,t_1t_2)-G^{cc}_{+-}(k,t_1t_2)\Sigma^{cv}_f(k_1t_2)+\int dt_3[\Sigma^{cc}_r(k,t_1t_3)G^{cv}_{+-}(k,t_3t_2)+\Sigma^{cv}_r(k,t_1t_3)G^{vv}_{+-}(k,t_3t_2)$$
$$+\Sigma^{cc}_{+-}(k,t_1t_3)G^{cv}_a(k,t_3t_2)+\Sigma^{cv}_{+-}(k,t_1t_3)G^{vv}_a(k,t_3t_2)$$
$$-G^{cc}_r(k,t_1t_3)\Sigma^{cv}_{+-}(k,t_3t_2)-G^{cv}_r(k,t_1t_3)\Sigma^{vv}_{+-}(k,t_3t_2)$$
$$-G^{cc}_{+-}(k,t_1t_3)\Sigma^{cv}_a(k,t_3t_2)-G^{cv}_{+-}(k,t_1t_3)\Sigma^{vv}_a(k,t_3t_2)]\ . \tag{1}$$

Here, the band energies $\varepsilon_\nu(k)$ ($\nu=c,v$) are solutions of the Hartree-Hamiltonian, i.e., they describe the in-plane GaAs energy bands, which in our model are merely shifted by the amount δ as a result of the induced electric field (see Sec. V),

$$\varepsilon_c(k)=\frac{(\hbar k)^2}{2m_c}+E_g+\delta_c\ ,\quad m_c>0\ ; \tag{2}$$

$$\varepsilon_v(k)=\frac{(\hbar k)^2}{2m_v}+\delta_v\ ,\quad m_v<0\ . \tag{3}$$

The masses are understood to be the appropriate in-plane masses of the Γ point, which are listed in Table I. The label v denotes either the hh or the lh band and E_g is the energy gap for the corresponding valence-band–to–conduction-band (v-c) transition. The dipole energy

$$\Sigma_f(k,t)=-\mu^{cv}_k E_0(t)e^{-i\omega_0 t} \tag{4}$$

includes the optical field with central frequency ω_0 [$E_0(t)$ is a slowly varying envelope] and the dipole matrix element μ^{cv}. At this stage the light field in Eq. (4) includes both the excitation and the probe field. Besides G^{cv}_{+-} and the retarded and advanced Green's functions denoted by G_r and G_a, Eq. (1) contains the functions G^{cc}_{+-} and G^{vv}_{+-} which describe the carrier occupations of the bands c and v, respectively. The corresponding self-energies Σ result from the Coulomb interaction between the carriers. In the screened-Hartree-Fock approximation (SHF) $\Sigma(t_1t_2)$ is essentially given by $W(t_1t_2)G(t_2t_1)$, where W is the dynamically screened Coulomb interaction. The exact form of Σ used in the derivation of the generalized Wannier equation will be given at the end of this section.

In a general nonequilibrium situation, one would have to calculate the distribution functions of the carriers generated by the applied pump field under the influence of the relevant scattering processes. The analysis in this paper will, however, be restricted to the case of a thermal quasiequilibrium, where the carriers are assumed to be distributed according to Fermi functions normalized to the given densities. As described in Ref. 18, the probe spectrum is obtained from Eq. (1) by linearizing with respect to the probe field. Neglecting coherent pump-probe scattering effects, which are unimportant on the nanosecond time scales considered here, Eq. (1) remains formally unchanged in such a linearization process. However, the one-particle energies and distribution functions are now those of the excited system, whereas G^{cv}_{+-} is the response to the weak probe field.

The dependence of $G(t_1t_2)$ on the two times t_1 and t_2 is equivalent[12] to a dependence on the so-called macroscopic time T,

$$T=\frac{t_1+t_2}{2}$$

and the microscopic time t,

TABLE I. Parameters used in the calculations. The in-plane mass $m_\parallel$ and the masses in the z direction $m_\perp$ are given in units of the free-electron mass. The band-gap energies are given in eV. The conduction-band- to valence-band-offset ratio used is 0.67.

	GaAs	AlAs
$m_{e\perp}-\Gamma$	0.0666	0.15
$m_{e\parallel}-\Gamma$	0.0665	0.15
$m_{e\perp}-X_z$	1.3	1.1
$m_{e\parallel}-X_z$	0.19	0.19
$m_{e\perp}-X_{xy}$	0.19	0.19
$m_{e\parallel}-X_{xy}$	1.3	1.1
$m_{\mathrm{hh}\perp}$	0.34	0.752
$m_{\mathrm{hh}\parallel}$	0.1	0.1
$m_{\mathrm{lh}\perp}$	0.094	0.16
$m_{\mathrm{lh}\parallel}$	0.2	0.2
E_g^Γ	1.514	3.110
E_g^X	1.981	2.240

$$t = t_1 - t_2 \ .$$

In thermal equilibrium the Green's function can only depend on the time difference t. In the simplest case of noninteracting particles we have

$$G^{\nu\mu}_{+-}(k,t) = G^{\nu\mu}_{+-}(k,\, t=0)\exp\left[-\frac{i}{\hbar}\frac{\varepsilon_\nu(k)+\varepsilon_\mu(k)}{2}t\right] , \tag{5}$$

$$i\hbar G_r^{\nu\mu}(k,t) = \delta_{\nu\mu}\Theta(t)\exp\left[-\frac{i}{\hbar}\varepsilon_\nu(k)t\right] . \tag{6}$$

In particular, the retarded Green's function of free particles in band ν oscillates as function of t with the energy of the respective band states. This corresponds to a pole of the Fourier transformed Green's function $G(k,\omega)$ at the particle energy $\varepsilon_\nu(k)$. We note that

$$i\hbar G^{\nu\nu}_{+-}(k,\, t=0) = f^\nu(k)$$

is the distribution function of carriers in band ν, and

$$i\hbar G^{cv}_{+-}(k,\, t=0) = P(k)$$

is the optical polarization function. If an external field is applied that breaks the time invariance of the system, all functions depend also on the macroscopic time T. The response to an optical field, i.e., the optical spectrum, is obtained from the Fourier analysis of

$$i\hbar G^{cv}_{+-}(k,\, t=0,\, T) = P(k,T)$$

with respect to T. As already mentioned, we are dealing in this paper only with the situation of quasithermal equilibrium, i.e., we assume that the T dependence of the polarization P is only due to the weak probe field. The distribution functions f are not altered by the probe field, and hence are assumed to be simple Fermi functions without any macroscopic time dependence.[1-3] We proceed as usual by transforming all functions H ($=G$ or Σ) which are nondiagonal in the Bloch band indices into the rotating frame

$$H^{cv}(t,T) = e^{-i\omega_0 T}\tilde{H}^{cv}(t,T) \ , \tag{7}$$

and Fourier transform Eq. (1) from t to ω.

For completeness we give the explicit form of the SHF self-energy[15]

$$\begin{aligned}\Sigma_r^{\nu\nu}(k,\omega) &= -i\hbar\sum_{k'}\int\frac{d\omega'}{2\pi}[W_a(k'-k,\omega'-\omega)G^{\nu\nu}_{+-}(k',\omega') \\ &\quad + W_{+-}(k'-k,\omega'-\omega)G_r^{\nu\nu}(k',\omega')] \\ &\quad + \delta_{\nu,v}\sum_{k'} V_{k'} \ , \end{aligned} \tag{8}$$

$$\Sigma^{\nu\nu}_{+-}(k,\omega) = i\hbar\sum_{k'}\int\frac{d\omega'}{2\pi}W_{-+}(k'-k,\omega'-\omega)G^{\nu\nu}_{+-}(k',\omega') \ , \tag{9}$$

$$\Sigma^{\nu\nu}_{-+}(k,\omega) = -i\hbar\sum_{k'}\int\frac{d\omega'}{2\pi}W_{+-}(k'-k,\omega'-\omega)G^{\nu\nu}_{-+}(k',\omega') \ . \tag{10}$$

The corresponding expression for $\tilde{\Sigma}^{cv}$ is obtained by replacing $G^{\nu\nu}$ with $\tilde{G}^{cv}$. Here V_q denotes the Coulomb potential between charge carriers in the limit of vanishing plasma density, and W is the corresponding potential dynamically screened by the excited hole and/or electron plasma. Explicit expressions for V and W will be given in the following section.

III. DYNAMICAL SCREENING

In this section we briefly describe our treatment of the screened Coulomb potential W. Since screening is a consequence of the intraband scattering of carriers as well as the emission and absorption of plasmons, the ω dependence of W generally ensures the energy conservation in those scattering processes and describes the statistical occupation of the scattering particles (e.g., the plasmons). Accounting for those dynamical processes leads to the problem associated with the Shindo approximation, as will be discussed in Sec. IV. Although a possible way to avoid this problem would be to treat the screening quasistatically,[1] we do not want to rely on the quasistatic approximation since we want to describe temperature-dependent damping mechanisms as realistically as possible.

In order to describe screening consistently for type-I and type-II systems, one needs a scheme which allows one to deal with cases where the electron and the hole densities vary independently. Therefore we extend the usual one-plasmon pole screening model, which approximates the contributions from the electron- and hole-pair-excitation continua by a single plasmon pole with an effective reduced mass, which is usually fitted in order to stabilize the exciton energy for all densities. The extension is a double-plasmon-pole model which is free of adjustable mass parameters.[19]

As is well known in equilibrium theory, the thermal occupation of the screening particles like plasmons is described by Bose functions n_B. The Keldysh approach contains the equilibrium formalism, and upon taking the thermal-equilibrium limit of the SHF approximation the $(+-)$ components of the screened potential include the Bose function n_B similar to the way the $(+-)$ components of G include the Fermi functions f,

$$i\hbar W_{+-}(q\omega) = n_B(\omega)2\hbar\,\mathrm{Im}W_r(q\omega) \ , \tag{11}$$

$$i\hbar W_{-+}(q\omega) = -[1+n_B(\omega)]2\hbar\,\mathrm{Im}W_r(q\omega) \ . \tag{12}$$

Equations (11) and (12) show that W_{+-} is the propagator of Bosons with spectral peaks given by $\mathrm{Im}(W_r)$ at the energies of the screening particles. Note, however, that in the present theoretical framework no assumptions concerning the commutator properties of screening particles are made, since the screening particles are only defined by the poles of the screened potential W_r. Within the

random-phase approximation, the spectrum of W_r includes the interband pair excitation continua of the electrons and holes at large wave vectors q and, in the case of a quasi-two-dimensional system, also two acoustic plasmon branches $q \simeq 0$. A thorough discussion of the corresponding three-dimensional electron gas can be found in Ref. 5.

In the corresponding double-plasmon-pole approximation we have[19]

$$\mathrm{Im}W_r(q\omega) = -\pi \sum_{i=1,2} g_i[\delta(\hbar\omega-\hbar\omega_i)-\delta(\hbar\omega+\hbar\omega_i)]V_q \ , \tag{13}$$

with the plasmon weight functions

$$g_i = \pm\hbar\frac{\omega_i^2\omega_{\mathrm{pl}}^2+Y}{2\omega_i(\omega_1^2-\omega_2^2)} \ , \tag{14}$$

where "+" corresponds to $i=1$ and "−" to $i=2$. We have used the abbreviations

$$\omega_{1/2}^2 = \tfrac{1}{2}\{\omega_q^2 \pm [(\omega_{q,e}^2-\omega_{q,h}^2)^2+4\omega_{\mathrm{pl},e}^2\omega_{\mathrm{pl},h}^2]^{1/2}\} \tag{15}$$

for the squared dispersions of the two branches and

$$Y = \omega_{\mathrm{pl},e}^2(\omega_{\mathrm{pl},h}^2-\omega_{q,h}^2)+\omega_{\mathrm{pl},h}^2(\omega_{\mathrm{pl},e}^2-\omega_{q,e}^2) \ . \tag{16}$$

The square of the total plasmon dispersion (and analogous of the total plasma frequency) is

$$\omega_q^2 = \omega_{q,e}^2+\omega_{q,h}^2 \ , \tag{17}$$

where the individual plasmon dispersion for each band $j=e,h$ is

$$\omega_{q,j}^2 = \omega_{\mathrm{pl},j}^2\left[1+\frac{q}{\kappa_j}\right]+\left[\frac{\hbar q^2}{2m_j}\right]^2 \tag{18}$$

with

$$\omega_{\mathrm{pl},j}^2 = V_q q^2\frac{n_j}{m_j} \ . \tag{19}$$

Here j labels the bands in the electron-hole picture (as opposed to the valence- and conduction-band picture), i.e., it labels electrons in the conduction band and holes in the valence band with $m_h=-m_v$. Furthermore, κ_j is the screening wave vector, which for equilibrium distributions with chemical potential μ_j is

$$\kappa_j = V_q q\frac{\partial n_j}{\partial\mu_j} \ . \tag{20}$$

Note that we use Gaussian units and incorporate the background dielectric constant ε_0 of GaAs in the electric charge, i.e., $e^2=e_0^2/\varepsilon_0$ with the free-electron charge e_0.

For completeness, we wish to give the concrete expression of the Coulomb potential used in our numerical calculations. Although at this point we could still use the wave functions of the lowest subband, which we obtain by solving the Schrödinger-Poisson equation for the motion in z direction, we will show in Sec. V and in the corresponding discussion in Sec. VI that for typical densities the wave functions of the Γ state are well localized in the GaAs layers. For practical purposes, we thus use the eigenfunctions of a quantum well of thickness L and infinitely high barriers to write the unscreened Coulomb interaction as

$$V_q = \frac{2\pi e^2}{q}F(q) \ . \tag{21}$$

Here, the form factor $F(q)$ accounts for the fact that the Coulomb potential is the matrix element of the $l=1$ subband eigenfunctions ϕ_1, i.e.,

$$\begin{aligned} F(q) &= \int dz \int dz' |\phi_1(z')|^2 e^{-q|z-z'|}|\phi_1(z)|^2 \\ &= \frac{8}{(qL)^2+4\pi^2}\left[\frac{3qL}{8}+\frac{\pi^2}{qL}-\frac{(1-e^{-qL})4\pi^4}{(qL)^2[(qL)^2+4\pi^2]}\right] . \end{aligned} \tag{22}$$

IV. GENERALIZED WANNIER EQUATION

We are now in a position to complete our discussion of the time dependence of Eq. (1) and present the final steps of the derivation of the generalized Wannier equation. Since the so-called Shindo approximation[20,21,13,15] can lead to significant errors for a one-component plasma, we introduce an alternative to this approximation, which in bulk and type-I systems is usually used to describe the dynamic screening processes of the two-component plasma.

Although, concerning the macroscopic time scale the usual approximation of neglecting gradient expansions of G with respect to the macroscopic time T (see, e.g., Refs. 3 and 15, and for a general presentation Ref. 12) allows us to treat the screening as being instantaneous, the correlation of one-particle states is still coupled in the self-energy term to the correlation function of the interband transition through the t or ω dependence of Σ and G^{cv}. Hence the optical transition, although taking place at a certain time T with $t=0$, couples the renormalized states which would emit or absorb plasmons when propagating for a finite time t. This is not a contradiction, since the time scale of T is large in comparison with the lifetime of a one-particle state. In order to avoid the extremely involved task to solve two equations for G, one each for the T and the t dependence, one usually proceeds by making an ansatz for the t, or equivalently the ω dependence of G. For instance, the so-called Shindo approximation[20,13,15] treats the t dependence of G as being that of noninteracting particles in a steady-state light field with frequency ω_0. The t dependence of G is then chosen to be a prefactor g^0 of $G(t=0)$, where $G(t=0)$ is the ω-integrated G divided by 2π,

$$\tilde{G}_{+-}^{cv}(k,t,T) = g^0(k,t,T)\tilde{G}_{+-}^{cv}(k,\, t=0,\, T) \ . \tag{23}$$

The prefactor has to normalized such that

$$g^0(k,\, t=0,\, t)=1 \ . \tag{24}$$

The meaning of g^0 becomes more clear if formulated for the Fourier transformed quantity, i.e., given in terms of ω rather than t. The Shindo approximation is then derived from Eq. (1) by setting $\Sigma^{\mathrm{SHF}}=0$ (see e.g. Ref. 15), yielding

$$i\hbar\tilde{G}^{cv}_{+-}(k\omega T) = \left[\frac{f^v(k)}{f^v(k)-f^c(k)}2\pi\hbar\delta\left[\hbar\omega-\frac{\hbar\omega_0}{2}-\varepsilon^v(k)\right] - \frac{f^c(k)}{f^v(k)-f^c(k)}2\pi\hbar \times\delta\left[\hbar\omega+\frac{\hbar\omega_0}{2}-\varepsilon^c(k)\right]\right]P(k,T) . \quad (25)$$

A systematic but numerically involved improvement of this approximation which even includes the transition to an exact treatment of the ω dependence of G is discussed in Ref. 15. Within the Shindo approximation, G exhibits as a function of ω two poles, which have as a function of k the dispersions of the conduction and valence bands, respectively, and which are centered roughly in the middle of the energy gap (note: $\hbar\omega_0\simeq E_G$). The sum of the weights of these two poles is $2\pi\hbar$, so that indeed condition (24) is fulfilled, but each pole can have an infinite weight if $f^v(k)-f^c(k)$ vanishes. In a highly excited type-I system this happens only at the Fermi vector k_F. Since the total polarization is the integral of P over k, such a singular point does not have a large influence on the final result. However, in highly excited type-II systems f^v-f^c is zero for all states between 0 and k_F, since $f^c=0$ due to the electron transfer out of the layer and $f^v=1-f^h=0$ due to the occupation of the hole states. Therefore the Shindo approximation has to be avoided for highly excited type-II systems. Instead, we introduce an ansatz in the spirit of free particles, by using the t (or equivalently ω) dependence of Eq. (5). This yields only a single pole in the middle of the gap with a dispersion given by the average of the c and v bands,

$$i\hbar\tilde{G}^{cv}_{+-}(k,\omega,T)=2\pi\hbar\delta\left[\hbar\omega-\frac{\varepsilon^v(k)+\varepsilon^c(k)}{2}\right]P(k,T) . \quad (26)$$

In contrast to the Shindo approximation, this ansatz is even consistent with the usual ansatz for the Green's function which is diagonal in the Bloch indices, i.e.,

$$i\hbar G^{vv}_{+-}(k,\omega)=2\pi\hbar\delta(\hbar\omega-\varepsilon_v(k))f^v(k) . \quad (27)$$

Within the same approximation, we use

$$G_r^{vv}(k,\omega)=\frac{1}{\hbar\omega-\varepsilon_v(k)+i\gamma} \quad (28)$$

and

$$G_r^{cv}(k,\omega)=0 \quad (29)$$

to evaluate the right-hand side of Eq. (1). Here γ is a small positive number that ensures the retardation properties of G_r and may also phenomenologically account for damping and dephasing processes in the limit of vanishing excitation density. To attempt a self-consistent calculation of γ at high densities within a calculation of optical spectra exceeds our computational possibilities. Note, however, that the excitonic line broadening is due to the dynamical screening of the Coulomb potential, which is treated in the way discussed above.

Summarizing all our approximations, we obtain a closed equation for $P(k,T)$, including the distribution functions for electrons, holes, and plasmons, which in the following will be evaluated only for the case of a quasithermal equilibrium seen by the probe light field. After Fourier transforming from T or Ω the generalized Wannier equation for P is then

$$\left[\varepsilon^c(k)-\varepsilon^v(k)-\hbar\omega_0-\hbar\Omega-i\gamma+\sum_{k'}\{V_{k'-k}[f^v(k')-f^c(k')]-V_{k'}+V_{k'-k}[\chi^v_{k'k}-\chi^c_{k'k}]\}\right]P(k,\Omega) - [f^v(k)-f^c(k)]\sum_{k'}V_{k-k'}P(k',\Omega)-\sum_{k'}V_{k-k'}[\chi^v_{kk'}-\chi^c_{kk'}]P(k',\Omega)=\mu^{cv}_k E_0(\Omega)[f^v(k)-f^c(k)] , \quad (30)$$

with

$$\chi^v(k,k')=\sum_{i=1,2}g_i(k-k')\left[\frac{f^v(k)+n_B(\omega_i(k-k'))}{\varepsilon^v(k)-\Delta_{k'}+\hbar\omega_0/2-\hbar\omega_i(k-k')+i\gamma}+\frac{1-f^v(k)+n_B(\omega_i(k-k'))}{\varepsilon^v(k)-\Delta_{k'}+\hbar\omega_0/2+\hbar\omega_i(k-k')+i\gamma}\right] \quad (31)$$

and

$$\chi^c(k,k')=\sum_{i=1,2}g_i(k-k')\left[\frac{f^c(k)+n_B(\omega_i(k-k'))}{\varepsilon^c(k)-\Delta_{k'}-\hbar\omega_0/2-\hbar\omega_i(k-k')-i\gamma}+\frac{1-f^c(k)+n_B(\omega_i(k-k'))}{\varepsilon^c(k)-\Delta_{k'}-\hbar\omega_0/2+\hbar\omega_i(k-k')-i\gamma}\right] , \quad (32)$$

where $\Delta_k=[\varepsilon^c(k)+\varepsilon^v(k)]/2$ and the plasma dispersions ω_i and weight factors g_i are defined in Eqs. (15) and (14). The structure of Eq. (30) is formally identical to the well known Bethe-Salpeter equation for excitons discussed, e.g., in Ref. 13. The phenomenological dephasing or collision broadening rate γ models the scattering processes in the limit of vanishing density. These rates determine the finite spectral width of the exciton resonance observed in linear optical spectra.

In the limit of zero excitation density all exchange and screening contributions vanish and the remaining inhomogeneous equation yields a hydrogenlike exciton spectrum. At finite densities, Eq. (30) accounts for the effect of Pauli blocking through the phase-space factors f^v-f^c, as well as for the screening of the Coulomb potential due to the plasma which reduces the e-h attraction (off diagonal in k,k') and the band gap via the self-energy terms (diagonal in k,k'). Note, however, that the details of the

screening function χ are not the same as in the Shindo approximation. At this point, we want to stress once more that our alternative to the Shindo approximation is still on the same general level as the Shindo approximation in that it is a simple factorized ansatz for the ω dependence of G^{cv}.

The approximation of quasistatic screening can be recovered formally from Eqs. (31) and (32) by neglecting all energies except the plasmon dispersions $\hbar\omega_i$ in the energy denominators, i.e., by formally setting $\varepsilon^v(k)-\Delta_{k'}+\hbar\omega_0/2+i\gamma=0$ in Eq. (31) and correspondingly $\varepsilon^c(k)-\Delta_{k'}-\hbar\omega_0/2-i\gamma=0$ in Eq. (32). This yields the quasistatic approximation for a two-component plasma, i.e., it contains two independent plasma densities and plasmon dispersions. In the case of zero electron density (the ideal type-II case), the correct quasistatic screening of a one-component plasma is recovered, since in that case the two plasmon weight functions g_i reduce to 0 and $\hbar\omega_{\mathrm{pl},h}^2/2\omega_{q,h}$, respectively.

V. SPACE-CHARGE EFFECTS

We now consider the effects of the space charge set up by the spatially inhomogeneous plasma. To study the influence of the space-charge field on the optical spectra, we self-consistently solve the coupled Schrödinger and Poisson equations for the confined carriers in the quantum well. It has been shown that in type-I quantum-well systems these effects are rather small.[22] However, in type-II systems the charge separation can be expected to be much more significant, at least for some transitions. Using the local-density approximation, the effects of exchange and correlation energies on the subband structure have been studied for type-I heterostructures and doping superlattices.[6,10] Since in the preceding sections we have calculated the absorption changes of the GaAs layers including already the exchange and correlation effects using the Hartree wave functions $\phi(z)$ as basis set, we must not include the exchange-correlation energy in the following calculation of $\phi(z)$ (otherwise we would count the exchange-correlation energy twice).

In this section we have to use a much more complete band-structure model than that used in the preceding sections in order to verify our assumption that the wave functions for the Γ and the X states are indeed well localized in the GaAs and the AlAs layers, respectively, and to calculate the band-gap shift of the Γ-Γ transition accurately. Therefore we take into account the Γ and all three X states for the conduction bands, and the hh and lh states for the valence band. This allows us to determine the density regime in which the simple model employed in the preceding sections is indeed justified.

Our numerical study consists of a self-consistent solution of the one-particle Schrödinger equation for the motion in z direction and of the corresponding Poisson equation. The z dependent potential entering the Schrödinger equation has contributions from (i) the potential profile U_0 caused by the different band gaps and band offsets between the different layers, and (ii) the induced potential U_{ind} due to the spatial charge separation. The induced potential is found by solving the Poisson equation, where the source term (i.e., the charge density) is obtained by filling up the one-particle states determined by the Schrödinger equation according to quasiequilibrium Fermi functions. In detail, the eigenstates of the Γ, X_{xy}, X_z electrons and the heavy and light holes all have to be found as solution of the Schrödinger equation

$$\frac{\hbar^2}{2}\frac{d}{dz}\frac{1}{m_j(z)}\frac{d}{dz}\phi_{jl}(z)+[U_{0j}(z)\pm U_{\mathrm{ind}}(z)]\phi_{jl}(z)=\varepsilon_{jl}\phi_{jl}(z)\ , \tag{33}$$

where l denotes the subband index and j indicates the Γ and X state for electrons and hh and lh states for holes, respectively. Note that throughout this section we use the electron-hole picture rather than the valence-conduction-band picture, so that all hole masses and energies are obtained from the corresponding valence-band quantities by multiplying with -1. The masses in Eq. (33) are the z masses listed in Table I. The plus sign refers to holes and the minus sign to electrons, respectively. The given density n of electrons and holes is distributed between the subbands according to Fermi statistics, with the appropriate density of states (i.e., in-plane masses) for each subband. Note that for the total structure the densities of electrons and holes are always equal, only within the individual layers the electron and hole densities can be different. For the electrons we have

$$n=\sum_l \sum_{j=\Gamma,X_z,X_{xy}} n_{jl}^e\ , \tag{34}$$

with

$$n_{jl}^e=2\sum_k \frac{1}{\exp\left[\beta\left(\frac{\hbar^2k^2}{2m_j}+e_{jl}^e-\mu_e\right)\right]+1}\ , \tag{35}$$

where the factor of 2 accounts for the Kramers degeneracy. μ_e is the chemical potential of the electrons and e_{jl}^e denotes the density-dependent energy of the bottom of the (l,j) conduction band. The Fermi functions contain the in-plane masses (Table I). Correspondingly, we have for the holes

$$n=\sum_l \sum_{j=\mathrm{hh,lh}} n_{jl}^h\ , \tag{36}$$

with

$$n_{jl}^h=2\sum_k \frac{1}{\exp\left[\beta\left(\frac{\hbar^2k^2}{2m_j}+e_{jl}^h-\mu_h\right)\right]+1}\ . \tag{37}$$

The charge density at a given position is obtained by summing the product of the square of the wave function and the population over each subband. This is the source term for the Poisson equation for the space-charge potential

$$\frac{d^2U_{\mathrm{ind}}}{dz^2}=4\pi e^2\left[\sum_{\substack{j=\Gamma,X_z,X_{xy};\\ l}} n_{jl}^e|\phi_{jl}(z)|^2-\sum_{\substack{j=\mathrm{hh,lh};\\ l}} n_{jl}|\phi_{jl}(z)|^2\right]\ . \tag{38}$$

Since experimentally used heterostructures consist of many layers, we employ periodic boundary conditions in the solution of Eqs. (33) and (38). We look for solutions at the reduced zone center, i.e., the wave functions repeat every supercell period such that $\phi(z+L)=\phi(z)$.

As mentioned above, our approach to treat the local plasma effects separately within each layer is based on the assumption that we can factorize the one-particle wave functions into a part depending only on x,y and a z-dependent part. Solving Eqs. (33) and (38), we can prove at least *a posteriori* that such a factorization is piecewise possible if the various wave functions are restricted to certain regions, in our case the single layers. Since it turns out that the Γ wave function, which in the structures under consideration are the relevant wave functions influencing the optical absorption process, are indeed well localized in the GaAs layer, our method to calculate the absorption in the GaAs layer only is consistent.

We numerically solved the coupled Schrödinger and Poisson equations (33) and (38) with the material parameters given in Table I for a structure with an AlAs layer width of 80 Å and a 29-Å GaAs layer. In Fig. 2 we show the resulting band-gap shift for the direct and indirect transitions as functions of the excitation density. Since the main voltage drop of the induced potential $U_{\rm ind}$ occurs between adjacent layers, it affects mostly the $\Gamma-X$ transition which determines the indirect luminescence. An example of $U_{\rm ind}$ and of the square of the wave functions $\phi(z)$ for the density $n=10^{12}$ cm^{-2} is shown in Fig. 3. The consequences for the luminescence spectra have been discussed in Ref. 11. The induced potential has its maxima and minima in the middle of the single layers and therefore it does not lead to a pronounced difference of the spatially direct transitions, as shown in Fig. 2. The fact that we still find a slight shift for this transition, in this case toward higher energies, is solely due to the difference in z masses and potential barriers for the electrons and the holes. These small differences may, however, strongly depend on the model for the zero-density potential U_0 which we take to be a square well. The general

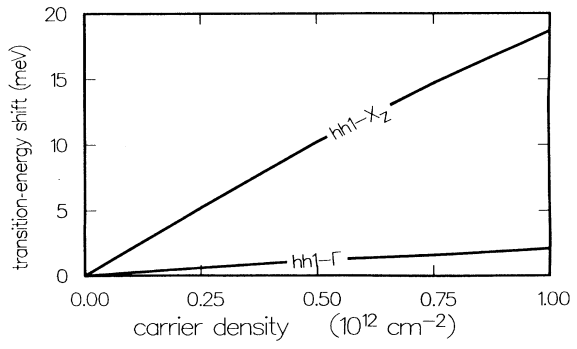

FIG. 2. Density-dependent increase of the optical Γ-Γ and Γ-X transition as a consequence of the electric field which is induced by the charge separation in a type-II structure. Shown is only the transition from the lowest heavy-hole subband.

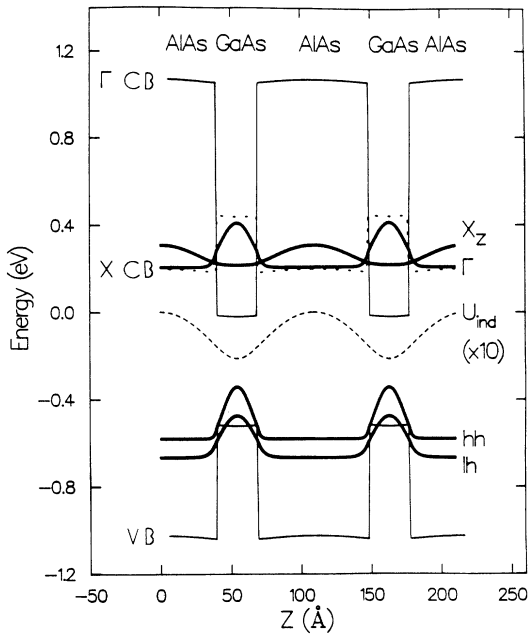

FIG. 3. Self-consistently calculated z dependence of the Γ- and X-point energies in a type-II structure for a carrier density of 10^{12} cm^{-2}. Also shown is the induced potential $U_{\rm ind}$ and the squares of the lowest subband wave functions of the heavy and light holes at Γ and electrons at Γ and X.

result, however, that for a given density the Γ-Γ transition shift due to $U_{\rm ind}$ is much less than the exchange self-energy shift is not sensitively dependent on the model for U_0.

In addition to the shifts of the energy levels, we have to consider the reduction of the excitonic oscillator strength which is proportional to the square of the overlap matrix element

$$\int dz\, \phi_{1,e}(z)\phi_{1,h}(z)\ ,$$

where both wave functions belong to the Γ point. In the conventional quantum confined Franz-Keldysh effect (see, e.g., Refs. 1 and 4) an externally applied field leads to a reduction of the e-h overlap integral and hence to a reduction of the excitonic oscillator strength. The case considered here is different in that the voltage drop occurs mostly between adjacent layers and less so within one layer. Furthermore, the fact that we are dealing with extremely narrow GaAs layers also reduces possible modifications caused by the electric fields. The numerical evaluation of the overlap matrix elements shows that in the relevant density regime the optical spectra are not influenced by the small reduction of e-h overlap. For carrier densities less than 10^{12} cm^{-2} the matrix element changes less than 1%.

VI. ABSORPTION SPECTRA

In this section we discuss our numerical solutions of the generalized Wannier equation (30) which yields the

absorption spectra of a single GaAs layer. Since we can neglect macroscopic electric field effects for the type-II structures under consideration, the main difference between type-I and type-II systems in our model is the amount of electrons in the GaAs layer compared to the occupation of holes. In the following, we show results for the situation of $n_e = n_{\rm hh}$ and $n_{\rm lh} = 0$, i.e., a type-I system in which the hh-lh splitting exceeds the chemical potential of the hole, so that the lh occupation can be neglected. Furthermore, we discuss the case where $n_e = 0$, i.e., an ideal type-II system with complete charge transfer. We also analyze the situation where only a certain fraction of electrons contributes to the screening and/or the phase-space filling in the GaAs layer. The material parameters used are the in-plane masses as given in Table I, the bulk-exciton binding energy $E_R = 4.2$ meV and the corresponding bulk-exciton Bohr radius 140 Å. The phenomenological dephasing rate γ is taken to be $0.6E_R$, corresponding to a dephasing time T_2 of 260 fs. This dephasing rate leads to a relatively broad but still well-resolved exciton of the nonexcited structure. At the same time the chosen rate takes into account the enhanced dephasing in type-II systems due to the rapid charge transfer.[8] This parameter choice allows us to compare type-I and type-II results for exactly identical input parameters. A more realistic choice of γ for the different situations, i.e., a larger one for type-II systems and room-temperature type-I systems and a smaller one for low-temperature type-I systems, would only have a minor effect on the homogeneous spectra as discussed in the following, and even less so on the inhomogeneously broadened spectra.[11,23]

Figure 4 shows absorption spectra of a type-II system (i.e., $n_e = 0$) for different excitation densities and a temperature of $T = 30$ K. The relatively low density of $n_{\rm hh} a_B^2 = 0.2$ ($\simeq 10^{11}$ cm^{-2}) shows essentially no shift of the hh resonance. This corresponds to the fact, well known for type-I and bulk systems, that at low densities the reduction of the band gap cancels very well the reduction of the binding energy of the exciton.[1,2,13] This cancellation is less exact in the case of the lh exciton. Here we have no phase-space filling at all, leaving only the screening caused by the hh plasma. Although this reduces the binding energy of the lh exciton, this reduction is overcompensated by the so-called Debye shift or Coulomb hole shift of the lh band gap. In a quasistatic approximation this Debye shift would be the difference between the screened and the bare Coulomb potential.[1] Figure 4 shows this small redshift and saturation of the lh exciton with increasing hh density. At the same time we see in the hh region the transition to the case of the so-called Burstein shift. In an ideal case of noninteracting particles at $T = 0$ this shift reflects the fact that for $n_e = 0$ the absorption vanishes in the energy range between the band gap and the Fermi level of the holes. In our more realistic calculation this situation is characterized by the shrinkage of the band gap with increasing density, the Coulomb enhancement in the absorption region, and the additional damping or dephasing processes caused by the hh plasma. The fact that the band-gap shrinkage is always sublinear with density ($\simeq n^{1/2}$), whereas the chemical potential approaches a linear increase at higher densities, leads to an effective blueshift of the absorption edge. This is the Burstein shift for a type-II system, and the absorption peak above the chemical potential is generally known as Coulomb enhancement peak or Mahan exciton.[1-4]

In Fig. 5 we investigate the effect of a higher hh plasma temperature. We see that the increased temperature causes different modifications of the hh and lh resonances. In the case of the hh transition, the effects of

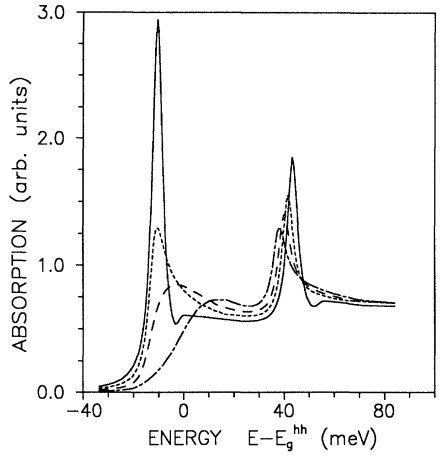

FIG. 4. Excitonic absorption spectra of a highly excited type-II structure for various densities n (in units of a_B^{-2}): 0 (solid line), 0.2 (short-dashed line), 0.4 (long-dashed line), and 0.8 (dash-dotted line). The linear ($n = 0$) spectrum shows two exciton peaks which correspond to the lowest subband of the heavy-hole and light-hole exciton, respectively. The plasma temperature is 30 K.

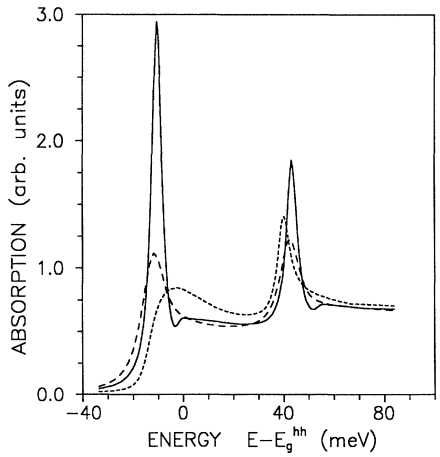

FIG. 5. Excitonic absorption spectra of a highly excited type-II structure for various temperatures: 300 K (long-dashed line) and 30 K (short-dashed line). The density is $0.4a_B^{-2}$. The solid shows the linear spectrum.

Pauli blocking, which are responsible for the Burstein shift in Fig. 4, are strongly reduced. The high-temperature plasma yields only a broadened exciton, which is slightly redshifted at low densities. This redshift is again well known for the case of type-I or bulk systems and it reflects the fact that in order to compute a constant exciton energy, one needs strong phase-space filling contributions. As a rule of thumb one might say that the compensation of the band gap reduction and the reduction of the exciton binding energy is slightly incomplete if regarded separately for the screening contributions to Eq. (30) and the phase-space contributions. Whereas this incomplete compensation leads to a redshift in the case of screening only and to a blueshift for pure phase-space filling effects, the combination of the two contributions usually yields the constant exciton position. Only if the balance of these contribution is altered or even destroyed, which is the case in Fig. 5 for the lh exciton as well as for the hh exciton, an exciton shift is to be expected. The change of this balance in favor of the phase-space filling effects has been discussed in the context of low-density low-temperature exciton gases in narrow type-I structures.[24,25] In general, the screening caused by an exciton gas is weaker than the screening by a plasma. In addition, screening in a two-dimensional (2D) system is generally weaker than in a 3D system, so that indeed the balance between screening redshift and phase-space-filling blueshift might be broken in a 2D exciton gas.

In order to investigate the effects of the dynamical screening used in this paper, we show in Fig. 6 a comparison of the hh spectra of Fig. 5 with corresponding results obtained within the quasistatic screening model. The low-temperature spectra do not depend drastically on the exact screening model. This is expected since the phase-space filling, not the screening, is the strongest plasma contribution. The high-temperature spectra are more strongly influenced by details of the used model for Coulomb screening. The comparison of the dynamically screened spectrum with the quasistatically screened one shows that the latter exhibit an appreciable redshift of the exciton resonance. This redshift, well known from bulk and type-I structure calculations, is usually assigned to the overestimation of screening within the quasistatic model. We should note, at this point, that in the present case of a single-component plasma there is no ambiguity of the asymptotic behavior of the plasmon dispersion at large q since it has to approach the intraband pair continuum of the holes, see Eq. (18). Thus, in contrast to the two-component plasma case, we cannot easily amend the quasistatic model to reduce the redshift. In comparison, our dynamic calculation shows exciton bleaching but no pronounced shift.

For the calculations of type-I systems we restrict ourselves to densities above the Mott density, so that the possibility of an exciton condensation is ruled out from the beginning. The simple reason for such a restriction lies in the extreme numerical complication associated with the exact solution of Eq. (30) in the case of exciton systems. These complications are a consequence of the fact that the one-particle distribution functions can no longer be chosen to be Fermi functions, but have to be determined self-consistently from the solution of generalized semiconductor Bloch equations.[1-4] A simple example for this situation arises in a slightly different context, namely in the optical Stark effect, where, upon neglecting all screening contributions, it can be shown that in the low density limit $f(k)$ is given by $|P(k)|^2$. In the context of the two-level atoms this is nothing but the conservation of the Bloch vector.

Results for a type-I system are shown in Fig. 7, where we have chosen the same parameters as in Fig. 4. Here, the lowest density shown yields already a very small gain

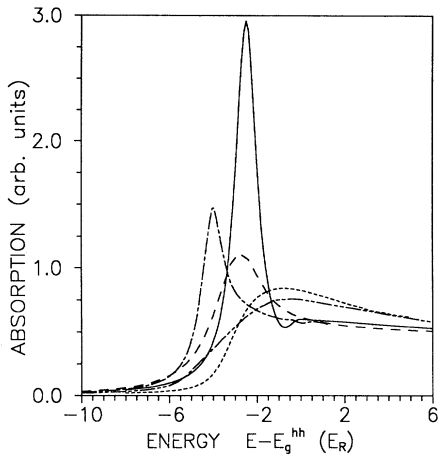

FIG. 6. Comparison of dynamical and quasistatic screening for the hh contribution of Fig. 5. The long-dashed line is the hh spectrum of Fig. 5 at $T=300$ K and the dashed-dotted line is the corresponding spectrum obtained within the quasistatic approximation. The short-dashed line is the 30-K hh spectrum of Fig. 5 and the dashed–double-dotted line is the corresponding quasistatic spectrum. The solid line shows the linear hh spectrum. E_R is the exciton Rydberg in bulk GaAs (4.2 meV).

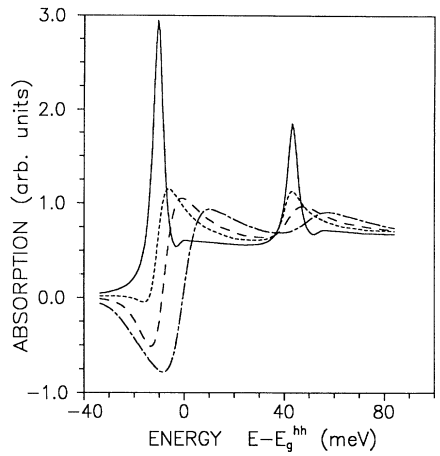

FIG. 7. Same as in Fig. 4, but for a type-I structure.

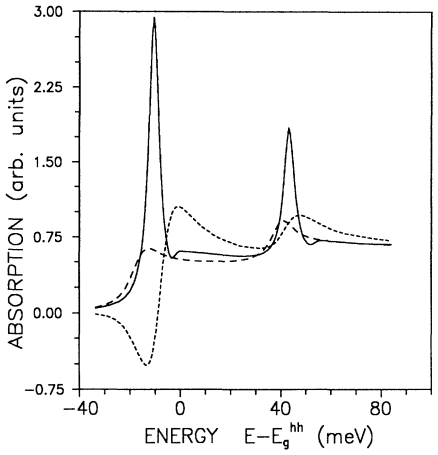

FIG. 8. Same as in Fig. 5, but for a type-I structure.

region for the hh transition, thus being clearly above Mott density. The blueshift of the corresponding Coulomb enhancement peak at the absorption onset originates from the same density dependence of the band-gap shrinkage and chemical potential discussed above. As in the case of the type-II system, even the highest density shown exhibits a significant Coulomb enhancement peak. In contrast to the type-II spectra, this peak cannot be confused with a shifted exciton peak since it is accompanied by the gain region at lower densities. However, the question if this argument still holds true in the more realistic case of inhomogeneously broadened spectra still has to be discussed.[23] Concerning the lh exciton, we observe in Fig. 7 a constant peak position at low densities and a strong blueshift at high densities. This behavior has formally the same origin as the behavior of the hh resonance in the type-II case. The only difference is that now the electron states are occupied and the hole states, in this case the light holes, are empty, whereas in the type-II situation the heavy-hole states are occupied and no electrons are present.

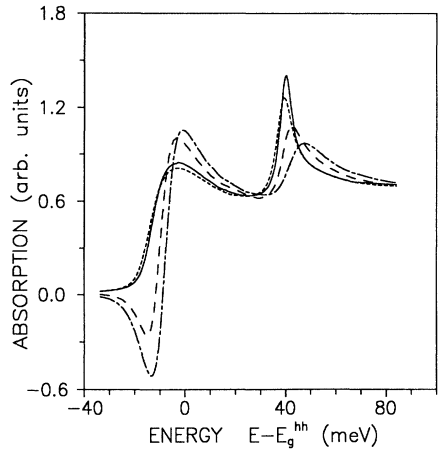

FIG. 9. Excitonic absorption spectrum for $n_e = \frac{1}{2} n_{hh}$ with $n_{hh} = 0.4 a_B^{-2}$ (long-dashed line). Also shown for the same densities is the case, where the electrons contribute only to the screening, not to the phase-space filling (short-dashed line). For comparison, the limiting case $n_e = n_{hh}$ (dashed-dotted line) and $n_e = 0$ (solid line) are shown. The temperature is 30 K.

Figure 8 shows that a significant temperature increase affects the type-I spectra quite similarly as the type-II spectra. The gain region decreases or even vanishes since the higher temperature significantly broadens the carrier distributions. The lh exciton is now more bleached and slightly redshifted.

In order to investigate the situation of a nonideal type-I or type-II structure, we have plotted in Fig. 9 solutions for the case where the electron density is half the hh density. We distinguish here two cases. First, we look at a simple nonideal charge transfer where the electrons remain in the Γ band of the GaAs layer, hence taking part not only in the plasma screening but also in the phase-space filling. As can be expected, the resulting spectrum is halfway between the corresponding type-I and type-II spectra. The second possibility of a nonideal system is that the electrons contribute only to the screening but not to the phase-space filling. This models the case when the X electrons are not completely localized in the AlAs layer, i.e., the wave function $\phi(z)$ for the X electrons has a tail into the GaAs layer. Figure 9 shows that an additional electron screening without electronic phase space filling has very little effect on the hh spectrum and leads only to a slightly increased redshift of the light hole.

VII. CONCLUSIONS

In summary, we presented a theoretical investigation of the nonlinear absorption of highly excited type-I and type-II quantum-well structures. Our analysis is based on a plasma theory which accounts for dynamical charge-carrier correlations, but which avoids the so-called Shindo approximation. We evaluated the theory numerically, focusing on the parameter regions where the hh states are occupied and the lh states are empty. In this parameter regime, a type-I spectrum that shows gain in the vicinity of the hh exciton corresponds to a type-II spectrum, which exhibits a blueshifted Mahan exciton. The corresponding lh exciton exhibits a blueshift in the type-I case because the Fermi edge of the electrons shifts to higher energies, whereas in the type-II case the lh exciton experiences only a minor redshift and loss of oscillator strength because of the plasma screening due to the hh plasma.

To demonstrate our theoretical results we presented in this paper exclusively homogeneously broadened spectra. Realistic heterostructures with thin quantum wells, however, always exhibit well-width fluctuation leading to quite pronounced inhomogeneous broadening of the optical spectra. For a comparison of our theoretical spectra with experimental data it is therefore crucial to account for this inhomogeneous broadening.[23]

ACKNOWLEDGMENTS

We are indebted to G. Olbright for his cooperation in the field of type-II structures. Stimulating discussions and collaborations with H. M. Gibbs, G. Khitrova, N. Peyghambarian, and R. Pon are also acknowledged. This work was supported by grants from the NSF, Optical Circuitry Cooperative (University of Arizona), U.S. Army Research Office, and U.S. Air Force Office of Scientific Research (JSOP), Sandia National Laboratories, and by a grant for CPU time at the Pittsburgh Supercomputer center. R. B. acknowledges support from the Deutsche Forschunggemeinschaft (DFG).

*Present address: Philips Research Laboratories, Redhill, Surrey RH1 5HA UK.

[1]H. Haug, and S. Schmitt-Rink, Prog. Quantum Electron. **9**, 3 (1984); H. Haug and S. W. Koch, *Quantum Theory of the Optical and Electronic Properties of Semiconductors* (World Scientific, Singapore, 1990).

[2]R. Zimmermann, *Many-Particle Theory of Highly Excited Semiconductors* (Teubner Texte zur Physik, Leipzig, 1987), Vol. 18.

[3]*Optical Nonlinearities and Instabilities in Semiconductors,* edited by H. Haug (Academic, London, 1988).

[4]S. Schmitt-Rink, D. S. Chemla, and D. A. B. Miller, Adv. Phys. **38**, 89 (1989).

[5]L. Hedin and S. Lundqvist, in *Solid State Physics: Advances in Research and Applications,* edited by F. Seita, D. Turnbull, and H. Ehrenreich (Academic, New York, 1969), Vol. 23, p. 1.

[6]T. Ando, A. B. Fowler, and F. Stern, Rev. Mod. Phys. **54**, 437 (1982).

[7]P. Dawson, B. A. Wilson, C. W. Tu, and R. C. Miller, Appl. Phys. Lett. **48**, 541 (1986); K. J. Moore, G. Duggan, P. Dawson, and C. T. Foxon, Phys. Rev. B **38**, 5535 (1988).

[8]J. Feldmann, R. Sattmann, E. O. Göbel, J. Kuhl, J. Hebling, K. Ploog, R. Muralidharan, P. Dawson, and C. T. Foxon, Phys. Rev. Lett. **62**, 1892 (1989); J. Feldmann, J. Nunnerkamp, G. Peter, E. Göbel, J. Kuhl, K. Ploog, P. Dawson, and C. T. Foxon, Phys. Rev. B **42**, 5809 (1990).

[9]H. W. van Kesteren, E. C. Cosman, P. Dawson, K. J. Moore, and C. T. Foxon, Phys. Rev. B **39**, 13 426 (1989); P. Dawson, C. T. Foxon, and H. W. van Kesteren, Semicond. Sci. Technol. **5**, 54 (1990).

[10]P. Ruden and G. Döhler, Phys. Rev. B **27**, 3538 (1983).

[11]G. R. Olbright, J. Klem, A. Owyoung, T. M. Brennen, R. Binder, and S. W. Koch, J. Opt. Soc. Am. B **7**, 1473 (1990); G. R. Olbright, W. S. Fu, A. Owyoung, J. F. Klem, R. Binder, I. Galbraith, and S. W. Koch, Phys. Rev. Lett. **66**, 1358 (1991).

[12]L. P. Kadanoff and G. Baym, *Quantum Statistical Mechanics* (Benjamin, New York, 1962).

[13]R. Zimmermann, K. Kilimann, W. D. Kraeft, D. Kremp, and G. Röpke, Phys. Status Solidi B **90**, 175 (1978).

[14]L. V. Keldysh, Zh. Eksp. Teor. Fiz. **47**, 1515 (1964) [Sov. Phys.—JETP **20**, 1018 (1965)].

[15]W. Schäfer and J. Treusch, Z. Phys. B **63**, 407 (1986).

[16]K. Henneberger, G. Manske, V. May, and R. Zimmermann, Physics A **138**, 577 (1986).

[17]L. D. Landau and E. M. Lifschitz, *Lehrbuch der Theoretischen Physik, Vol. X (Physikalische Kinetik)* (Akademie Verlag, Berlin, 1983).

[18]S. Schmitt-Rink, D. S. Chemla, and H. Haug, Phys. Rev. B **37**, 941 (1988).

[19]W. Schäfer, R. Binder, and K. H. Schuldt, Z. Phys. B **70**, 145 (1988).

[20]K. Shindo, J. Phys. Soc. Jpn. **29**, 287 (1970).

[21]W. Schäfer, in *Festkörperprobleme (Advances in Solid State Physics),* edited by U. Rössler (Vieweg, Braunschweig, 1988), Vol. 28, p. 63.

[22]G. Livescu, D. A. B. Miller, D. S. Chemla, M. Ramaswamy, T. Y. Chang, N. Snuer, A. C. Gossard, and J. H. English, IEEE J. Quantum Electron. **QE-24**, 1677 (1988).

[23]G. R. Olbright, W. S. Fu, J. F. Klein, H. M. Gibbs, G. Khitrova, R. Pon, B. Fluegel, K. Meissner, N. Peyghambarian, R. Binder, I. Galbraith, and S. W. Koch, Phys. Rev. B **44**, 3043 (1991); K. Meissner, B. Fluegel, R. Binder, S. W. Koch, G. Khitrova, and N. Peyghambarian, Appl. Phys. Lett. **59**, 259 (1991).

[24]N. Peyghambarian, H. M. Gibbs, J. L. Jewell, A. Antonetti, A. Migus, D. Hulin, and A. Mysyrowicz, Phys. Rev. Lett. **53**, 2433 (1984).

[25]S. Schmitt-Rink, D. S. Chemla, and D. A. B. Miller, Phys. Rev. B **32**, 6601 (1985).